Complex modifier landscape underlying genetic background effects

Jing Hou[a,1], Guihong Tan[a], Gerald R. Fink[b], Brenda J. Andrews[a,1], and Charles Boone[a,1]

[a]Donnelly Centre for Cellular and Biomolecular Research, University of Toronto, Toronto, ON M5S 3E1, Canada; and [b]Whitehead Institute for Biomedical Research, Cambridge, MA 02142

Edited by Jasper Rine, University of California, Berkeley, CA, and approved February 4, 2019 (received for review December 7, 2018)

The phenotypic consequence of a given mutation can be influenced by the genetic background. For example, conditional gene essentiality occurs when the loss of function of a gene causes lethality in one genetic background but not another. Between two individual *Saccharomyces cerevisiae* strains, S288c and Σ1278b, ∼1% of yeast genes were previously identified as "conditional essential." Here, in addition to confirming that some conditional essential genes are modified by a nonchromosomal element, we show that most cases involve a complex set of genomic modifiers. From tetrad analysis of S288C/Σ1278b hybrid strains and whole-genome sequencing of viable hybrid spore progeny, we identified complex sets of multiple genomic regions underlying conditional essentiality. For a smaller subset of genes, including *CYS3* and *CYS4*, each of which encodes components of the cysteine biosynthesis pathway, we observed a segregation pattern consistent with a single modifier associated with conditional essentiality. In natural yeast isolates, we found that the *CYS3*/*CYS4* conditional essentiality can be caused by variation in two independent modifiers, *MET1* and *OPT1*, each with roles associated with cellular cysteine physiology. Interestingly, the *OPT1* allelic variation appears to have arisen independently from separate lineages, with rare allele frequencies below 0.5%. Thus, while conditional gene essentiality is usually driven by genetic interactions associated with complex modifier architectures, our analysis also highlights the role of functionally related, genetically independent, and rare variants.

conditional gene essentiality | background effect | complex modifier interactions | rare variants

Genetic backgrounds can impact the phenotypic consequences of a specific mutation and might constitute an inherent feature of biological traits, complicating our ability to predict individual phenotypes from genomic information (1–9). In many human Mendelian disorders, including cystic fibrosis, sickle cell anemia, and neurofibromatosis, even though the causal variant is well established (1, 10–13), individuals carrying the same causal mutation either do not always develop the disease, a phenomenon called incomplete penetrance, or do not display the same clinical symptoms, an effect known as variable expressivity. Variable penetrance or expressivity of a trait typically reflects environmental or genetic background influences and significantly impacts the ability to connect genotype to phenotype in natural populations (14).

While genetic background effects are commonly observed, the underlying molecular mechanisms remain mostly unknown. In general, genetic variants contributing to background effects are termed "modifiers." Identification of critical modifiers is difficult, likely due to the low population frequencies of the modified trait and the heterogenic nature of the modifiers involved (7, 15). In addition, recent evidence suggests that many genetic background effects are caused by highly complex modifier interactions, which themselves can be confounded by other genetic and environmental factors (5, 16–19). As a result, only a handful of examples of modifiers involved in human Mendelian diseases, notably in cystic fibrosis, have been identified (4, 10, 12, 13).

Recent large-scale comparative screens in many model systems, including yeasts, nematodes, *Drosophila*, mice, and human cell lines, have revealed an extensive catalog of background effects, mainly related to differential fitness consequences of well-defined loss-of-function mutations across genetically distinct individuals (20–30). In the budding yeast, *Saccharomyces cerevisiae*, we carried out a comparative study of systematic gene deletions in two closely related individuals, S288c and Σ1278b, and showed that in this context, ∼1% (57 genes) of all yeast genes are conditional essential, where the deletion of a given gene is lethal in one background but not another (23). These data provide an opportunity to systematically dissect the modifiers involved in background-specific phenotypes related to gene deletion variants. In addition, an important advantage of the yeast model is the availability of a large number of genetically diverse natural isolates. So far, the genomes of over 1,000 wild yeast isolates originating from various ecological and geographical locations have been completely sequenced (31). Combining these resources, the yeast model offers a unique opportunity to explore specific cases of conditional essentiality in two defined genetic backgrounds, and then to expand the analysis to the population level to discover variant frequency, type, and trait predictability.

Here, we characterized the modifier complexity involved in previously identified conditional essentiality cases between S288c

Significance

Genetic background impacts the phenotypic outcome of a mutation in different individuals; however, the underlying molecular mechanisms are often unclear. We characterized genes exhibiting conditional essentiality when mutated in two genetically distinct yeast strains. Hybrid crosses and whole-genome sequencing revealed that conditional essentiality can be associated with nonchromosomal elements or a single-modifier locus, but most involve a complex set of modifier loci. Detailed analysis of the cysteine biosynthesis pathway showed that independent, rare, single-gene modifiers, related to both up- and downstream pathway functions, can arise in multiple allelic forms from separate lineages. For several genes, we also resolved complex sets of modifying loci underlying conditional essentiality, revealing specific genetic interactions that drive an individual strain's background effect.

Author contributions: J.H. and C.B. designed research; J.H. performed research; G.T. and G.R.F. contributed new reagents/analytic tools; J.H., G.R.F., B.J.A., and C.B. analyzed data; and J.H., B.J.A., and C.B. wrote the paper.

The authors declare no conflict of interest.

This article is a PNAS Direct Submission.

Data deposition: The sequence reported in this paper has been deposited in the GenBank database (accession no. PRJNA493856).

[1]To whom correspondence may be addressed. Email: jing.hou@utoronto.ca, brenda.andrews@utoronto.ca, or charlie.boone@utoronto.ca.

This article contains supporting information online at www.pnas.org/lookup/suppl/doi:10.1073/pnas.1820915116/-/DCSupplemental.

Published online February 25, 2019.

and Σ1278b. We mapped the genomic regions involved in a subset of cases and focused on a pair of genes, *CYS3* and *CYS4*, which are involved in the cysteine biosynthesis pathway and are essential in Σ1278b but not S288c. We characterized and functionally validated the modifier underlying the Σ1278b-specific essentiality and expanded our analysis to other natural isolates. By surveying a large number of strains, we showed that cysteine biosynthesis pathway essentiality can be caused by variation in two independent modifiers, *OPT1* and *MET1*, that are linked to upstream or downstream pathway functions. Sequence analyses revealed that allelic variants of the identified modifiers independently arose from separate lineages and were extremely rare across the population.

Results

The Modifier Complexity of S288c/Σ1278b Conditional Gene Essentiality. We previously compared growth phenotypes of gene deletion mutant collections constructed in two laboratory strains, S288c and Σ1278b, and identified a total of 57 genes as conditional essential, among which 13 were specific to S288c and 44 were specific to Σ1278b (23). To select cases for modifier analysis, we first reanalyzed the conditional essential phenotype by tetrad dissection for all 57 candidates in heterozygous strains that carry a single deletion copy, both in the S288c and Σ1278b diploid backgrounds. Candidates that showed an incorrect segregation pattern (not 2:2 alive: dead, 13 strains; see Dataset S1), an unusual deletion locus (shorter or longer than expected deletion size, five strains; see Dataset S1), or severe loss of fitness in the nonessential background were not further analyzed (seven strains; see Dataset S1). In total, 32 out of the original 57 conditional essential genes satisfied our rigorous criteria for further assessment of mechanisms of conditional essentiality (Dataset S1).

To simplify the identification of the modifiers involved, we generated S288c/Σ1278b hybrids with deletions of both copies of the conditional essential gene and analyzed the segregation patterns of the surviving offspring. The construction of homozygous deletion hybrid required mating the viable haploid deletion mutant to the nonviable haploid deletion mutant in the conditional essential background. To do so, individual haploid deletion mutant cells from the viable background were placed in close proximity with the nongerminated spores originating from a diploid strain that was heterozygous for the corresponding conditional essential gene in the nonviable background (Fig. 1*A*). In yeast, spores carrying an inviable deletion allele can be rescued through a process of germination and immediate mating with a viable cell carrying a dominant modifier. Compared with a traditional transformation-based method, the rescue mating may minimize selective pressure due to marker selection and could potentially reduce the chance of acquiring de novo suppressors during the selection procedure. As there is no prior knowledge of the mating types for the nongerminated spores at the moment of tetrad dissection, we expect at most half of the spores can mate and form a zygote. Following this procedure, the resultant zygotes were manually isolated, approximately half of which were expected to be homozygous for deletion at the targeted locus. Using this strategy, we successfully obtained 22 S288c/Σ1278b diploid hybrids that were homozygous for deletion of a conditional essential gene and all 32 S288c/Σ1278b hybrids that were heterozygous for deletion of a conditional essential gene. However, 15 out of 22 homozygous deletion hybrids showed sporulation deficiency and were not analyzed further (Dataset S1). In total, our initial strain characterization identified seven homozygous deletion strains and 32 heterozygous deletion strains as S288c/Σ1278b hybrid diploids for subsequent tetrad analysis to identify modifiers.

As observed previously for S288c/Σ1278b hybrids (19), we confirmed that hybrids with heterozygous deletion of any one of six genes, *PEP12*, *PEP7*, *PHO88*, *SKI7*, *VPS34*, *VPS16*, displayed a 2:2 segregation pattern of viable progeny, with the deletion marker cosegregating with the lethal phenotype. Previous work showed that this segregation pattern reflects conditional essentiality associated with cytosolic factors related to the mitochondrial genomes and/or the presence of killer viruses (19). For 6 other cases, including *CYS3* and *CYS4*, we observed a segregation pattern that was consistent with a single modifier associated with the conditional essential gene. In the single-modifier cases, either a 2:2 segregation pattern in the homozygous deletion hybrid or a predominance of tetrads containing four, three, or two viable spores in the heterozygous deletion hybrid was observed, indicative of a single-modifier origin (Dataset S1). For the other 20 cases listed in Dataset S1, the segregation patterns in either heterozygous S288c/Σ1278b hybrid alone or both heterozygous and homozygous S288c/Σ1278b hybrids together indicate complex modifier origins, which is consistent with the general conclusion of our previous preliminary findings based on tetrad analysis (23).

Depending on the interaction patterns among the modifiers, the number of modifiers involved in some of the complex cases could be inferred from the segregation analyses. For example, in the case of *LSM6*, which encodes a component of a complex involved in RNA metabolism and processing, we predominantly observed tetrads with four, three, or two viable spores in the homozygous deletion hybrid, suggesting that two modifiers are likely involved, and the presence of either one can rescue the conditional essential phenotype associated with the deletion of *LSM6* (*SI Appendix*, Fig. S1*B* and Dataset S1). It is worth noting that other types of tetrads with either one or zero viable spores were also observed in this case, suggesting additional modifiers with possibly weaker effects may be involved. In the cases of *SWI6* and *OST4*, which encode a transcription factor and an oligosaccharyl-transferase component, respectively, a severe loss of offspring viability (~10% viable spores) was observed and only tetrads with one or two viable spores could be obtained after tetrad dissection of the sporulated homozygous deletion hybrids. In this scenario, at least three modifiers could be involved, with rescue of the conditional essential phenotype requiring the simultaneous presence of all modifiers (*SI Appendix*, Fig. S1 *C* and *D* and Dataset S1). Thus, there is no specific modifier that can act as a suppressor of the conditional essential phenotype; rather there is a complex set that must interact together. For other cases with more complex interaction patterns, segregations alone cannot predict the precise number of modifiers involved, especially for cases where homozygous deletion hybrids were not available (Dataset S1).

For the seven cases where both heterozygous and homozygous hybrids were available, all of which were Σ1278b-specific conditional essentials, we performed more detailed studies, including bulk segregant analysis followed by whole-genome sequencing to map the genomic loci involved (Fig. 1*A*). For each case, on the order of 100–400 additional tetrads were dissected for the homozygous S288c/Σ1278b hybrids, and at least 50 different segregants were isolated from independent tetrads (Fig. 1*A*). We focused on those tetrads that contained only one or two viable spores, which were then pooled and sequenced (Fig. 1 *B*–*D* and *SI Appendix*, Fig. S1). We anticipated that the surviving individuals in tetrads with the least numbers of viable spores would carry allelic combinations that cover most of the modifiers involved, as lethal combinations were maximized in these types of tetrads (Fig. 1*D*). In addition, for three of the seven cases, we observed marked differences in terms of colony size across the viable offspring obtained from the homozygous hybrids, possibly indicating the presence of secondary modifiers that impact fitness rather than viability. For each of these cases, an additional segregant pool was selected with only low fitness individuals to map secondary modifier loci involved in fitness variation (Fig. 1*C*). Genomic regions enriched in opposite parental origins in

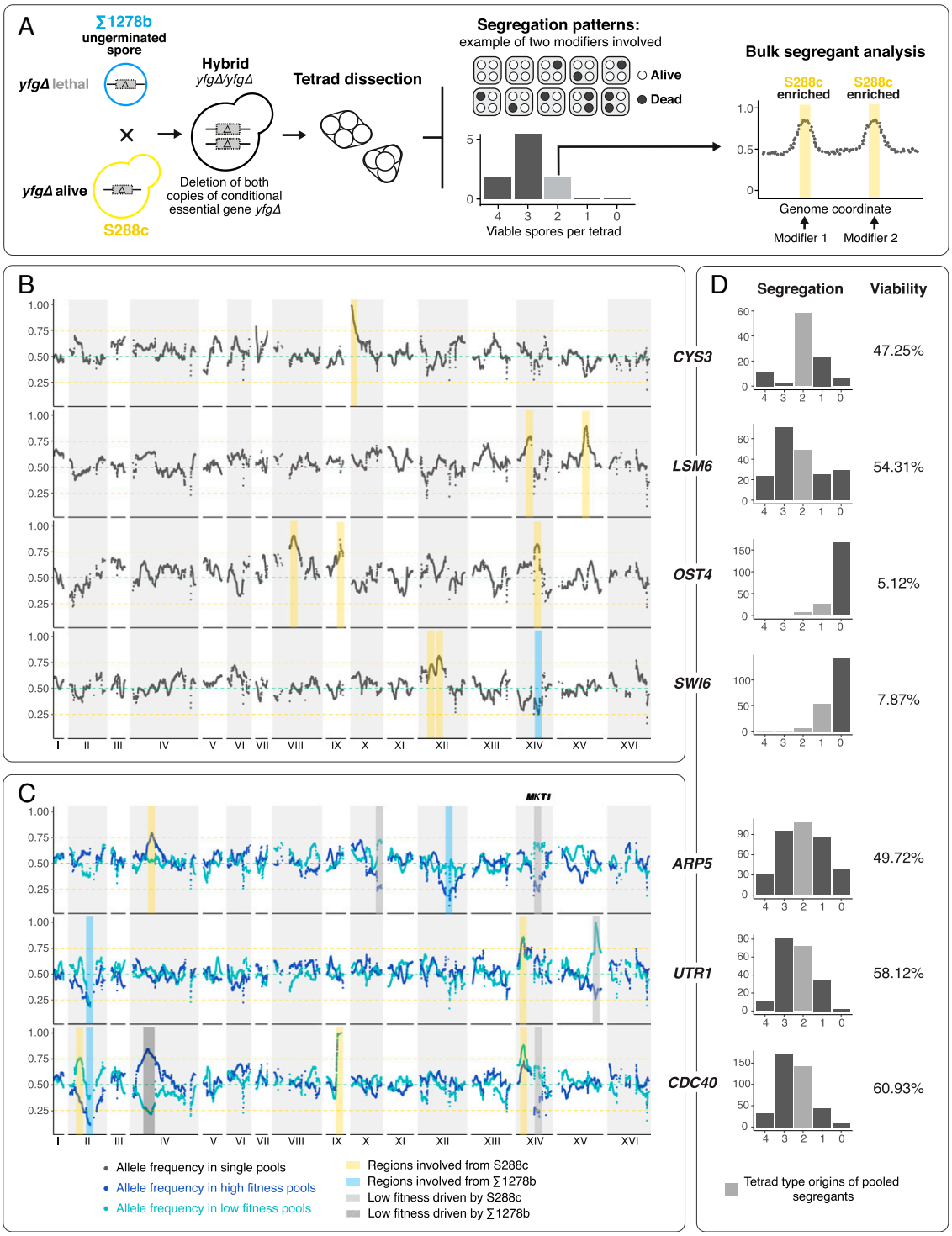

Fig. 1. Mapping of genomic regions involved in conditional gene essentiality cases between S288c and Σ1278b. (*A*) Schematic overview of the mapping strategy. S288c/Σ1278b hybrids homozygous for deletion of a conditional essential gene were generated by rescue mating in single nongerminated cells. Hybrids were then sporulated and tetrad dissections were performed to obtain segregation patterns of viable vs. inviable offspring in each tetrad. At least 50 offspring from independent tetrads were selected and the genomic regions involved were mapped using bulk segregant analysis followed by whole-genome sequencing. (*B*) Mapping results for segregant pools involving deletion of *CYS3*, *LSM6*, *OST4*, and *SWI6*. Genomic coordinates are indicated on the *x* axis and the allele frequency of S288c is indicated on the *y* axis. Dotted horizontal green lines indicate an allele frequency of 0.5 and the orange lines highlight allele frequencies of 0.75 and 0.25, as a visual aide. To simplify, kernel smoothed allele frequency within a 20-kb window is plotted. Shaded yellow bars highlight S288c-enriched regions and while blue bars indicate Σ1278b-enriched regions. (*C*) Mapping results for segregant pools involving *ARP5*, *UTR1*, and *CDC40*. The layout of the plots is described in *B*. For these pools, fitness variation was observed among the viable offspring, and two pools, one with higher fitness segregants indicated in dark blue and one with lower fitness highlighted in light blue, were sequenced. Gray shades indicate regions involved in fitness variation, as evidenced by the reversed enrichment directionalities between the high and low fitness pools. (*D*) Segregation patterns and offspring viabilities observed for the mapped cases. Between 100 and 400 tetrads were dissected for each case. The *x* axis indicates the number of viable offspring per tetrad, and the *y* axis, the overall count of tetrads observed in each category. Pooled segregants were originated from independent tetrads highlighted in gray.

the high fitness vs. low fitness pools were considered as fitness related, whereas regions enriched in the same direction were considered as involved in viability (Fig. 1*C*).

In total, we identified 21 genomic regions with a marked skew of allele frequency (greater than 2.5× SDs from the mean allele frequency; lower threshold <0.30, higher threshold >0.75), among which 16 regions were related to viability and 5 related to fitness variation (Fig. 1 *B* and *C* and *SI Appendix*, Fig. S1). The number of regions mapped was in concordance with the segregation patterns and predicted complexity. Specifically, we mapped 1 region for the single-modifier case *CYS3*, 2 regions for *LSM6*, and 3 regions for *SWI6* and *OST4*, as expected (Fig. 1*B* and *SI Appendix*, Fig. S1 *A*–*D*). Most modifier regions mapped were biased toward S288c (13 of 16), with exceptions for regions on chromosome XIV (*SWI6*), chromosome XII (*ARP5*), and chromosome II (*UTR1* and *CDC40*) (Fig. 1 *B* and *C*). The overall bias toward S288c-specific regions was expected, since all mapped cases were conditional essential in the Σ1278b background, indicating there can be synthetic lethal modifier alleles in the Σ1278b background, and, conversely, the corresponding suppressor alleles in the S288c background.

A Single Modifier for *CYS3* and *CYS4* Conditional Essentiality. Across all analyzed cases, a pair of genes, *CYS3* and *CYS4*, were remarkable in that they exhibited low modifier complexity. Both genes function in the cysteine biosynthesis pathway, converting homocysteine to cysteine through a two-step reaction (32). *CYS3* and *CYS4* were essential only in the Σ1278b background, while *cys3*Δ and *cys4*Δ mutants exhibited a lower fitness phenotype on rich medium in S288c (Fig. 2*A*). Segregation analyses indicated a clear pattern of single-modifier origin, with a near perfect 2:2 segregation in the S288c/Σ1278b hybrid with homozygous deletion of *CYS3* and a 4:3:2 pattern in S288c/Σ1278b hybrids with heterozygous deletion for either *CYS3* or *CYS4* (note that a homozygous deletion hybrid of *CYS4* did not sporulate; see *SI Appendix*, Fig. S1*A* and Dataset S1). We used a *CYS3* homozygous deletion S288c/Σ1278b hybrid to map the modifier to a single region on the left end of chromosome X, with skewed allele frequency toward S288c near 100% (Figs. 1*B* and 2*B*). Further examination of the region yielded *OPT1* as the candidate modifier gene (Fig. 2*B*).

OPT1 encodes a transmembrane oligopeptide transporter, responsible for the cellular uptake of glutathione (33). As cysteine is one of the necessary precursors for glutathione biosynthesis, *OPT1* is therefore directly related to the downstream function of the cysteine biosynthesis pathway. Indeed, supplementing the media with both cysteine and glutathione was shown to be able to alleviate the lethality caused by *CYS3* or *CYS4* deletions. We examined the allelic versions of *OPT1* in both

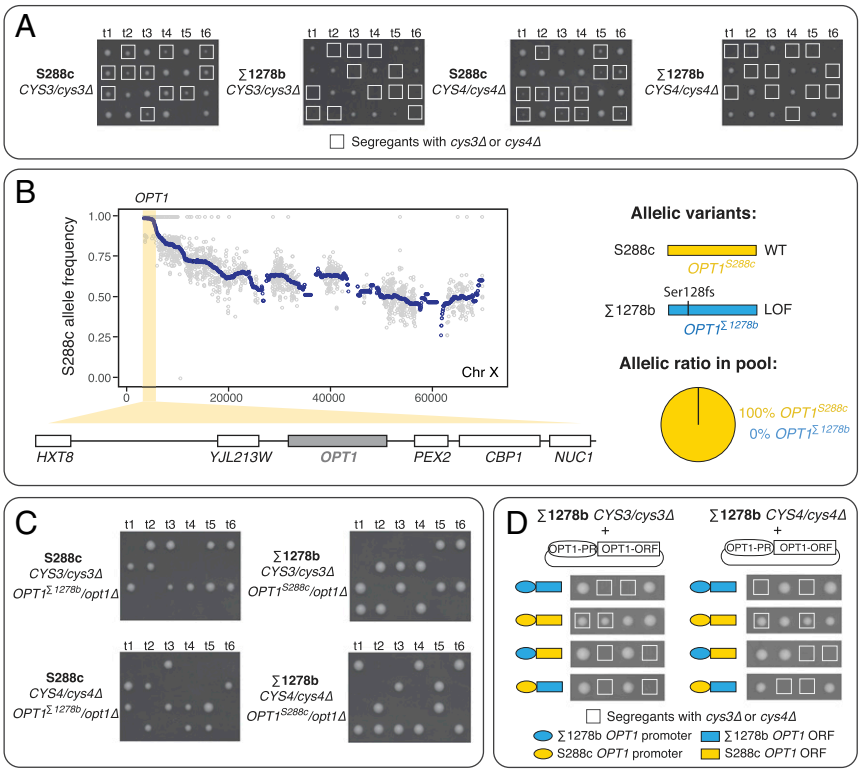

Fig. 2. Identification and functional validation of a modifier involved in *CYS3* and *CYS4* conditional essentiality between S288c and Σ1278b. (*A*) Essentiality of *CYS3* and *CYS4* in S288c and in Σ1278b. Diploids heterozygous for the indicated deletion allele were sporulated and tetrads dissection on rich medium. Segregants carrying the deletion are highlighted with squares. A total of six tetrads are presented for each case (t1–t6). (*B*) Allele frequency variation obtained from S288c/Σ1278b *cys3Δ/cys3Δ* segregant pool on chromosome X. Allele frequency of S288c is presented on the *y* axis and genomic coordinates on the *x* axis. The allele frequency of each polymorphic position between S288c and Σ1278b is plotted in gray and kernel smoothed average allele frequency in each 20-kb windows in blue. A significantly skewed region is highlighted in yellow, and genes located in this region are plotted. Allelic versions of the candidate *OPT1* genes are schematically presented on the *Right* side of the plot. The ratio of each of the parental *OPT1* allele is illustrated in the pie chart. Allele frequency variation across the whole genome is shown in Fig. 1*B* and *SI Appendix*, Fig. S1*A*. (*C*) Segregation patterns in *OPT1* allele replacement mutants in both S288c and Σ1278b backgrounds. The relevant genotypes of the mutant strains are indicated. (*D*) Rescue of *CYS3* and *CYS4* essentiality through ectopic expression of *OPT1* in Σ1278b. Centromeric plasmids carrying different combinations of S288c or Σ1278b promoter and protein encoding regions of *OPT1* were transformed into diploid Σ1278b heterozygous for deletion of *CYS3* or *CYS4*. Diploid transformants were sporulated and the tetrads obtained were dissected. The *OPT1* promoter-gene configuration is diagrammed to the *Left* of each tetrad and *cys3Δ* or *cys4Δ* segregants are indicated with a box. All tetrad dissections were performed on YPD.

S288c and Σ1278b and identified a single base pair insertion in Σ1278b, resulting in an early frameshift at amino acid position 128 (pSer128fs, full protein length 799; Fig. 2*B*). This mutation likely results in loss of function of *OPT1*, leading to a synthetic lethal phenotype with deletion of *CYS3* or *CYS4* in the Σ1278b background.

To validate this hypothesis, we generated a S288c diploid strain carrying a single deletion copy of *CYS3* or *CYS4*, with one copy of *OPT1* deleted and the other copy replaced with the Σ1278b version (S288c *CYS3*/*cys3Δ*, $OPT1^{\Sigma1278b}$/*opt1Δ*, and S288c *CYS4*/*cys4Δ* $OPT1^{\Sigma1278b}$/*opt1Δ*; Fig. 2*C*). We observed clear synthetic lethality between *opt1Δ* and *cys3Δ*, *opt1Δ* and *cys4Δ*, as well as between $OPT1^{\Sigma1278b}$ and *cys3Δ* or *cys4Δ*, indicating that the $OPT1^{\Sigma1278b}$ is a loss-of-function variant and is indeed involved in the conditional essentiality of *CYS3* and *CYS4* in the Σ1278b background.

However, we performed the reciprocal experiment in Σ1278b and discovered that the $OPT1^{S288c}$ allele failed to rescue the lethal phenotype in the presence of *cys3Δ* or *cys4Δ* (Fig. 2*C*). We suspected that the Σ1278b background might carry additional mutations in the promoter region of *OPT1*, resulting in a lack of rescue when only the protein encoding region was replaced. To test this idea, we expressed the different allelic versions of *OPT1* from either its S288C or Σ1278b promoter on a plasmid and found that only the S288c promoter with the S288c version of *OPT1* was able to rescue the lethality in Σ1278b in the presence of *Δcys3* or *Δcys4* (Fig. 2*D*). Sequence comparison identified three mutations in the Σ1278b *OPT1* promoter, a T > C substitution at position −108, a C > T at position −142, and a 1-bp deletion of a poly T sequence around position −148, potentially causing defects in promoter function (*SI Appendix*, Fig. S2*A*). Together, these results suggest that Σ1278b carries a loss-of-function allele of *OPT1* caused by variation in both the promoter and the ORF, leading to the conditional essentiality of the cysteine biosynthesis pathway in this background.

Survey of Cysteine Biosynthesis Pathway Essentiality Across Natural Yeast Populations. While we established that the cysteine biosynthesis pathway essentiality in Σ1278b can be due a single loss-of-function modifier *OPT1*, the prevalence and specificity of this conditional phenotype at the population level is unclear. As previous experiments showed that *CYS3* and *CYS4* behaved similarly in terms of disrupting the cysteine biosynthesis pathway function when deleted, we used *CYS3* as the indicator of pathway essentiality for subsequent analyses. To test for a *CYS3* conditional essential phenotype in other genetic contexts, we randomly sampled 23 additional yeast isolates originating from various ecological and geographical locations (Dataset S2) (34) and tested the essentiality of *CYS3* deletion in these backgrounds. We deleted a single copy of *CYS3* in the diploid individuals and quantified the fitness of the *CYS3* deletion mutants, by calculating the ratio between the colony sizes of segregants carrying the *cys3Δ* mutation and wild-type segregants in the same background, after tetrad dissection (median ratio from 20 mutants vs. 20 wild types) (Fig. 3*A*). The *CYS3* gene was not essential in most isolates, while the *cys3Δ* individuals in these backgrounds showed a similar lower fitness phenotype compared with that seen in the S288c background (Fig. 3*A*). However, we identified one background Y12, isolated from African palm wine, that required *CYS3* for viability (Dataset S2). Sequence analysis in Y12 did not reveal any apparent loss-of-function mutations in *OPT1*, indicating that this case might have an independent modifier origin. To test this hypothesis, we crossed Y12 with Σ1278b and subsequently generated hybrid diploids, each deleted for a single or both copies of the *CYS3* gene. Because we could make the hybrid Y12/Σ1278b diploid that was deleted for both copies of the *CYS3* gene, the conditional essential modifiers were highly likely to be different in the two genetic backgrounds. Indeed, we observed a 4:3:2 pattern for segregants derived from the heterozygous deletion hybrid and a 1:2:1 pattern for the homozygous deletion hybrid, suggesting that the Y12 conditional essentiality was due to a single modifier that is independent from *OPT1* (Fig. 3*B*).

To map the modifier involved, we selected 50 independent segregants originating from the Y12/Σ1278b *CYS3*/*cys3Δ* hybrid that carries the *cys3Δ* mutation but not the loss-of-function version of $OPT1^{\Sigma1278b}$. These segregants were pooled, sequenced, and the allele frequency of Y12 was scored (Fig. 3*C*). As expected, the allele frequencies at the *CYS3* and *OPT1* loci were enriched for Σ1278b and Y12, respectively (Fig. 3*C*). Based on the segregation analysis, we expected the Y12-specific *CYS3* essentiality to be due to a single modifier, independent of *OPT1*. Therefore, segregants that carried the *cys3Δ* and *OPT1-WT* alleles should also carry a Σ1278b allele, corresponding to the Y12-specific modifier. We observed a genomic region enriched for Σ1278b at the right end of chromosome XI, which likely contains the Y12-specific modifier. Detailed analysis of the region revealed *MET1* as the potential candidate (Fig. 3*C*). We also observed that a region on the left arm of chromosome XII was enriched for Y12 alleles. This Y12 enrichment may map a secondary modifier for fitness rather than viability, which should be associated with the Σ1278b sequence, such as those in the *MET1* region.

The *MET1* gene encodes a S-adenosyl-L-methionine uroporphyrinogen III transmethylase, which is involved in the biosynthesis of S-adenosyl-homocysteine, a precursor of homocysteine (Fig. 4*A*). Compared with Σ1278b, the Y12 version of *MET1* carries a nonsynonymous mutation at protein position 179, resulting in a histidine-to-glutamine substitution. The only other variation that seemed potentially relevant was a premature stop codon identified at position 592 (Leu592*, full length 593), leading to deletion of one amino acid at the end of the coding sequence, which seemed unlikely to impact protein function (Fig. 3*C* and *SI Appendix*, Fig. S2*B*). We performed allele replacement of *MET1* with the Σ1278b allelic version in diploid Y12 carrying deletions of both copies of *CYS3* (Fig. 3*D*). A single replacement of $MET1^{\Sigma1278b}$ rescued the lethality of *CYS3* deletion in Y12, confirming that *MET1* was indeed involved in the conditional essentiality of the cysteine pathway in this background (Fig. 3*D*). We note that a genomic survey across ∼1,000 wild yeast isolates (31) revealed that ∼90% of all strains carry the Leu592* allele, including most strains in our *CYS3* deletion test set. This observation shows that the Leu592* allele alone is not sufficient to cause the synthetic lethality.

Allelic Survey Reveals Additional Backgrounds for Cysteine Pathway Essentiality. The examples from Σ1278b and Y12 demonstrated that independent modifiers impacting functions both upstream and downstream of the cysteine biosynthesis pathway can lead to a background-specific essential phenotype. Due to the simple modifier complexity involved in these cases, we sought to predict the cysteine pathway essentiality across diverse *S. cerevisiae* isolates by surveying potential genomic variants that may carry similar modifier effects. We mapped out the pathway by including genes involved in both biosynthesis of homocysteine and glutathione, based on the modifier effects of *MET1* and *OPT1*, respectively (Fig. 4*A*), and looked for genomic variants related to all these genes across over 1,000 yeast genomes (31).

We first focused on the *MET1-H179Q* variant, specific to the Y12 background. We found an additional isolate, K12, that carries the exact same allelic variant. K12 is a heterozygous diploid strain isolated from Japanese Sake and belongs to the same lineage as Y12 (Fig. 4*B*). Despite heterozygosity at other loci in the genome, the *MET1-H179Q* variant is homozygous in K12. Deletion of a single copy of *CYS3* in K12 showed this gene was essential for viability (Fig. 4*C*). Furthermore, we performed the same experiment on another Japanese Sake isolate from the

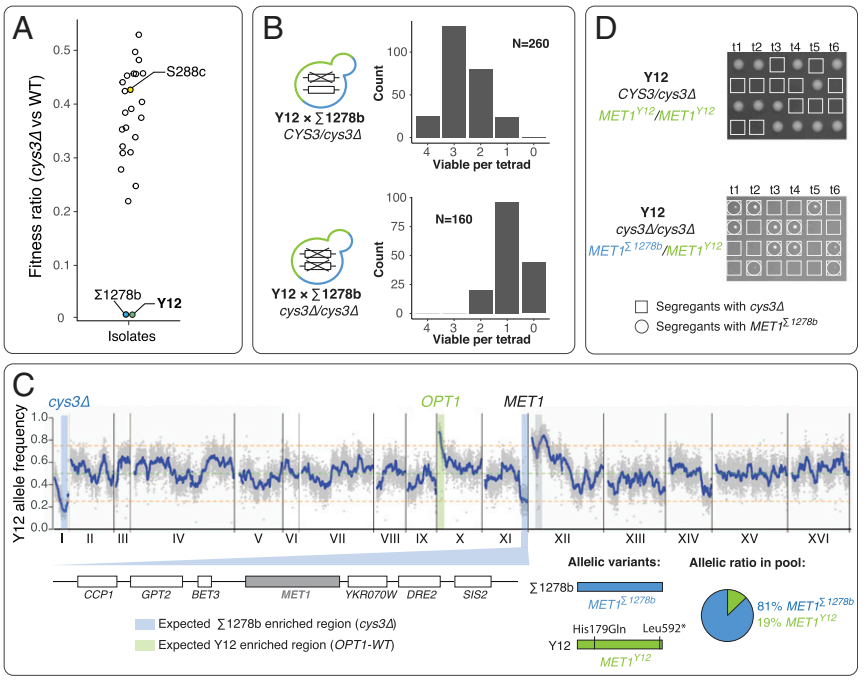

Fig. 3. An *OPT1*-independent *CYS3* conditional essential background identified through survey of natural yeast isolates. (*A*) Fitness ratio of *cys3Δ* in 25 yeast isolates with diverse origins. Fitness ratios were calculated as the ratio between colony sizes of *cys3Δ* mutant and wild-type individuals in their respective genetic backgrounds. The fitness ratios of S288c (yellow), Σ1278b (blue), and Y12 (green) are highlighted. (*B*) Segregation patterns for *CYS3* conditional essentiality in Σ1278b/Y12 hybrids. Σ1278b/Y12 hybrids heterozygous (*Upper* plot) or homozygous (*Lower* plot for deletion of *cys3Δ*) were sporulated and the segregation patterns of viable spores in the resulting tetrads are plotted. The number of tetrads for each tetrad type is indicated on the *y* axis (count), while the tetrad type is listed on the *x* axis. (*C*) Mapping of a Y12-specific modifier using bulk segregant analysis. A region with significantly skewed allele frequency toward Σ1278b on chromosome XI is highlighted, and the genes within the region are diagrammed below the plot. The allelic versions of the candidate modifier *MET1* are schematically presented and the ratio between the two parental alleles are plotted in the pie chart. (*D*) Functional validation of *MET1* modifiers using allele replacement. Segregation patterns for diploid Y12 heterozygous or homozygous for deletion of *CYS3* carrying the MET1Y12 or heterozygous for the $MET1^{\Sigma 1278b}$ are presented. Individuals with a *cys3Δ* are highlighted in squares and individuals carrying the replaced $MET1^{\Sigma 1278b}$ allele are highlighted in circles.

same lineage, K12_2, which does not carry the *MET1-H179Q* variant, and showed that *CYS3* was not essential in this background (Fig. 4*C*). These observations indicated that the *MET1-H179Q* variant was sufficient to predict cysteine pathway essentiality in other backgrounds.

In addition to the specific nonsynonymous *MET1* allele, we also surveyed for all potential loss-of-function variants, including premature stop codon, frameshift, and loss of start codon mutations, for all genes involved in the pathway (Fig. 4*A*). We did not find any loss-of-function variants associated with *SAM2*, *MET6*, or *SAH1*. Variants with premature stop codons were found for *SAM1*, *CYS3*, *CYS4*, *GSH1*, *GSH2*, and *MET1*, but only in isolates with high ploidy levels (from 3n to 5n) and the variants were exclusively in a heterozygous state. These observations suggest that the function of the cysteine biosynthesis pathway is highly conserved across the surveyed population.

Interestingly, we identified two additional loss-of-function variants associated with *OPT1*, which arose from independent lineages. The first one corresponds to a premature stop codon mutation at position 16 (Ser16*, full length 799), found in two isolates, 906 and 908, originating from Mexican agave, in a homozygous state (Fig. 4*B*). The second *OPT1* variant contained a premature stop codon at position 535 (Gln535*, full length 799), identified as homozygous in EXF-5837 and heterozygous in CLIB563 and CLB556, all isolates from French dairy material (Fig. 4*B*). We focused on isolates that were homozygous for the predicted modifier alleles, namely 906, 908, and EXF-5837, for subsequent analyses. To test the cysteine pathway essentiality in these backgrounds, we generated monosporic diploid segregants for each of the three strains and deleted a single copy of *CYS3*. As expected, a 2:2 segregation pattern was observed in all strains tested, indicating that the *CYS3* gene is indeed essential in these backgrounds (Fig. 4 *D* and *E*). As a control, we also tested *CYS3* essentiality in PW5, a strain that is genetically similar to the Mexican agave isolates 906 and 908 but does not carry the $OPT1^{Ser16*}$ allele, and showed that *CYS3* is not essential in this background (Fig. 4*D*). Overall, our results show that rare, multiple allelic variants can lead to cysteine pathway essentiality across different lineages within a yeast population.

Complex Modifier Architectures Underlying Conditional Gene Essentiality. In the case related to the cysteine biosynthesis pathway essentiality, we showed that independent modifiers, i.e., *OPT1* and *MET1*, with lineage-specific allelic variants, together drive the essentiality of this pathway across a population (Fig. 5*A*). In addition to this example, our mapping results indicate various types of modifier architecture can lead to conditional essentiality (Fig. 5 *B–D*). In the case of *LSM6*, a RNA metabolism and processing related gene, two genomic loci localize on chromosomes XIV and XV were mapped through the S288c/Σ1278b *lsm6Δ*/*lsm6Δ* hybrid, both of which were enriched for the S288c alleles (Fig. 1*B*). Based on the 4:3:2 segregation pattern, each one of these two loci was able to rescue the lethal phenotype (Fig. 5*B*).

In contrast to this simple architecture, the suppression of the essentiality in some cases requires the combined effect of multiple loci, involving combinations that originate from the same genetic background (i.e., a transcription factor *OST4*) (Fig. 5*C*) or novel allelic combinations derived from hybrid background (i.e., a oligosaccharyl-transferase component *SWI6*) (Fig. 5*D*). In

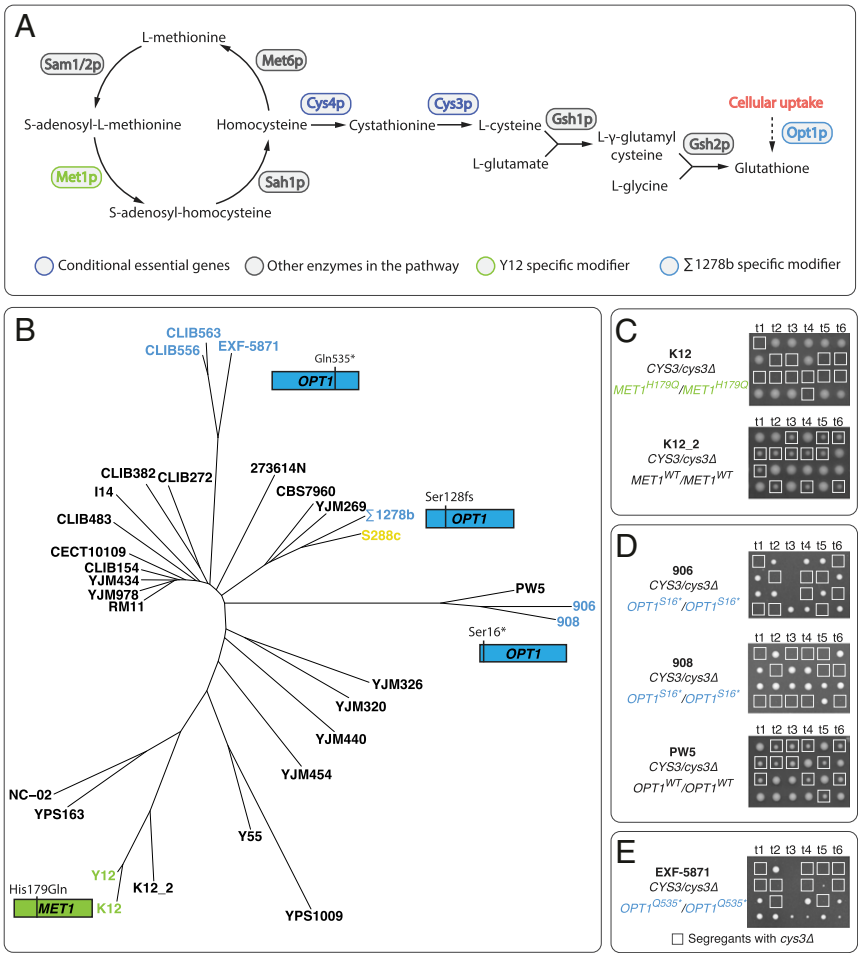

Fig. 4. Modifiers underlying the cysteine pathway essentiality arise from independent lineages. (*A*) Overview of genes involved in the cysteine biosynthesis pathway. Conditional essential and modifiers in the pathway are highlighted. (*B*) Neighbor-joining tree of 31 isolates used in this study based on whole-genome sequence data (31). The reference strain S288c is highlighted in yellow, and strains that carry modifier variants of *OPT1* or *MET1* are highlighted in blue and green, respectively. (*C*) Heterozygous *CYS3/cys3Δ* diploid isolate predicted to have *CYS3* essentiality due to the *MET1* modifier (K12) was sporulated and offspring viability for several tetrads is shown. The same experiment was performed for an additional isolate in the same lineage that does not carry the predicted modifier (K12_2). The *cys3Δ* individuals are highlighted in squares. (*D*) Heterozygous *CYS3/cys3Δ* diploid isolates of strains predicted to have *CYS3* essentiality due to the *OPT1-S16** modifier allele (906 and 908) were sporulated and offspring viability for representative tetrads is shown. The same procedure was carried out in PW5, which belongs to the same lineage but does not carry the modifier allele. (*E*) Heterozygous *CYS3/cys3Δ* diploid strain in the EXF-5871 background, which carry the *OPT1-Q53S** allele, was sporulated and the offspring viability for representative tetrads is shown.

the latter example, allele combinations that arose de novo in the hybrid progeny can lead to suppression of the lethal phenotype related to the Σ1278b-specific conditional essential gene. In fact, while most regions mapped related to viability (13/16, Fig. 1 *B* and *C*) were enriched for the S288c alleles as expected, Σ1278b-specific regions were also found to be determinant in several cases. Notably, a Σ1278b-specific region on chromosome II and a S288c-specific region on chromosome XIV appeared to be co-occurring in two independent cases, *UTR1*, which encodes a kinase that phosphorylates both NAD and NADH, and *CDC40*, which encodes a pre-mRNA splicing factor (Fig. 1*C*). The S288c-specific chromosome XIV region is enriched in a narrow ∼10-kb window and peaks at *BNI1*, an 8-kb gene which encodes a formin protein that is involved in actin cable assembly and polarized bud growth (35). Interestingly, the S288c *BNI1* allele appeared to be in linkage disequilibrium with a Σ1278b-specific region on chromosome II, and the enrichment of this genetic interaction was observed for the viable spore progeny pools with either high or low fitness, for both the conditional essentialities of *UTR1* and *CDC40*. This genetic interaction pattern suggests that the S288C *BNI1* region may combine with a Σ1278b-specific region on chromosome II to suppress the conditional essentiality associated with *UTR1* and *CDC40* deletion alleles.

In addition, in two of three cases with offspring fitness variation, *ARP5* and *CDC40*, the same fitness-related region on chromosome XIV was mapped, which contains the well-known master regulator *MKT1*, previously found to be associated with multiple growth phenotypes in yeast (36–40). Our results showed that this genomic region was enriched for the S288c alleles in the low fitness segregant pools, indicating that *MKT1* might also be involved as the secondary modifier in these cases (Fig. 1*C*). These observations highlight the multitude of different and complex genetic architectures involved in the background-dependent gene essentiality phenotype.

Discussion

In this study, we performed a global analysis of genetic modifiers and their interactions underlying conditional gene essentiality previously identified in two laboratory yeast strains, S288c and Σ1278b (23). Using segregation-directed mapping strategies, we identified over 20 genomic regions linked to seven conditional essential genes. Although most conditional essential genes we

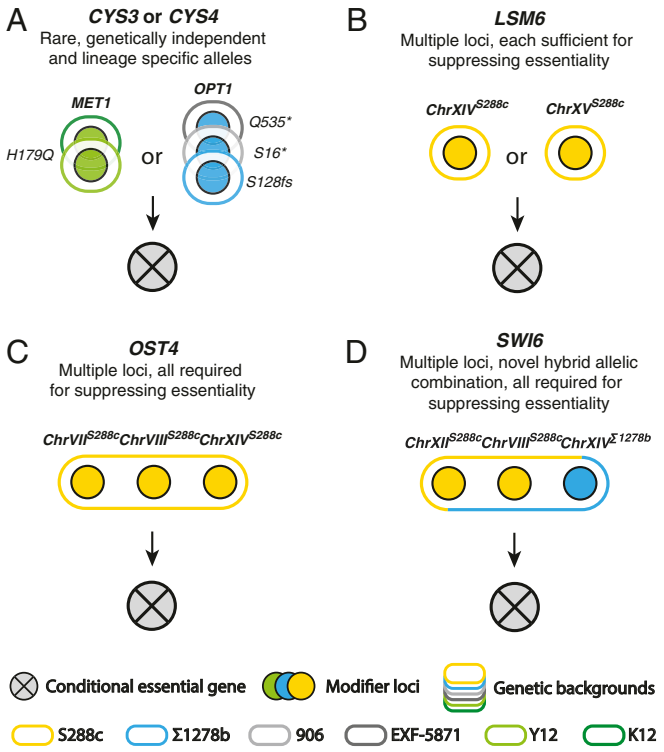

Fig. 5. Distinct types of modifier architecture involved in conditional essentiality. Colors indicate the genetic backgrounds from which the modifier loci were mapped (yellow, S288c; blue, Σ1278b; and green, Y12). Different genetic backgrounds are highlighted in color-coded ovals. Example cases for each proposed scenario are indicated at the *Top* of each panel. (*A*) Conditional essentiality related to independent genes and multiple allelic variants across different background. (*B*) Conditional essentiality related to independent loci in the same background, each locus alone is sufficient to suppress the lethal phenotype. (*C*) Combination of multiple loci in the same background suppress lethal phenotype. All loci are required simultaneously. (*D*) Novel allelic combination arose from hybrid of different strain backgrounds led to suppression of the lethal phenotype.

analyzed were associated with a complex set of modifiers, we characterized a single modifier that underlies conditional essentiality related to genes involved in the cysteine biosynthesis pathway. We examined the essentiality of the cysteine biosynthetic pathway across a large number of natural yeast isolates and identified two independent modifiers, *OPT1* and *MET1*, either of which could drive the conditional essential phenotype across separate lineages.

Conditional gene essentiality can be considered as an extreme example of the genetic background effect related to loss-of-function mutations and synthetic lethal genetic interactions, and is a widely observed phenomenon across different species. In addition to *S. cerevisiae*, conditional essential genes have been found in the fission yeast (20), *Caenorhabditis elegans* (25, 27, 28), *Drosophila* (10, 22), mouse (41), and human cell lines (21, 24, 26). So far, deeper characterization of the underlying genetic basis of conditional gene essentiality has only been explored in *S. cerevisiae*, and most cases appeared to involve complex modifier interactions across multiple genomic loci (23). However, in several cases, nonchromosomal elements, such as specific mitochondrial genomes and the presence of cytosolic killer viruses, can be involved in conditional essentiality (19).

Using more refined genomic mapping, we discovered that independent cases of conditional essentiality can be driven by modifiers with distinct genetic architectures (Fig. 5). On the one hand, the genetic suppression of the conditional essential phenotype can involve a single locus, with additional complexity due to the presence of different single modifier alleles in different backgrounds (e.g., *CYS3* and *CYS4*), or multiple modifier loci in the same background (e.g., *LSM6*). More commonly, the suppression of the essentiality requires the combined effect of multiple loci, involving combinations that originate from the same genetic background (e.g., *OST4*) or novel allelic combinations derived from hybrid backgrounds (e.g., *SWI6*) (Fig. 5). In the case of the novel allelic combinations, presumably this genetic solution to the conditional essential phenotype is simpler or associated with stronger suppression, such that it tends to dominate the viable hybrid spore progeny.

In particular, we observed that a novel hybrid combination of the S288c genomic region containing *BNI1* and a Σ1278b locus on chromosome II can impact the Σ1278b conditional essentiality of both *UTR1* and *CDC40*. This combination of loci is not found in either parent genetic background and shows that new genetic interactions in hybrid spore progeny can influence conditional essential phenotypes. In addition, secondary modifiers that contribute to fitness variation can also be involved (Fig. 1*C*). In total, we identified five fitness-related regions, among which four were unique to different gene deletions (Fig. 1*C*). By contrast, one specific region on chromosome XIV was mapped in two of three cases associated with fitness variation (*ARP5* and *CDC40*) (Fig. 1*C*). This region contains *MKT1*, a master regulator involved in various growth and expression traits, which has been repeatedly mapped in many quantitative trait loci studies in yeast (36–40), and is likely involved as a secondary modifier in several conditional essential cases.

While single modifier-driven cases are rare, they may be more likely to identify variants that are functionally related to the primary mutation (30). Indeed, our characterization of single gene modifiers of the cysteine biosynthesis pathway revealed that genes associated with functions both up- and downstream of the pathway can modify the essentiality of the primary pathway genes. However, our analysis of natural isolates revealed that allelic variants associated with the same modifier genes can arise independently from separate lineages, revealing layers of genetic complexity, even for apparently simple single gene modifiers. This observation emphasizes the need for multi-allelic analysis at the gene and pathway levels in genotype–phenotype correlation studies.

In the past few years, a wide variety of natural yeast isolates derived from various ecological and geographical niches has been fully sequenced, leading to a near-complete view of the genetic diversity within the *S. cerevisiae* species (31, 34, 42–44). Similar to human populations, the genomes of the natural yeast population carry a large number of rare variants, with over 80% of the total variants detected having a minor allele frequency of <5% (31). In fact, all functional variants previously identified through linkage mapping in yeast are rare variants across the population (31, 39, 40, 45, 46). Consistent with these studies, our analysis of conditional essentiality in the cysteine biosynthesis pathway identified functional modifier alleles with a frequency well below 5% within the population (*MET1-H179Q*, 0.2%; *OPT1-S128fs*, 0.05%; *OPT1-Q535**, 0.2%; and *OPT1-S16**, 0.2%). Together, these data suggest that rare variants may play an important role in phenotypic variation in yeast.

Compared with simple single-modifier cases, pinpointing the precise genes and mutations involved in conditional essentiality with complex genetic origins remains a nontrivial task. In part, the challenge is addressing the lethal phenotype associated with the conditional essential genes, which complicates classical genetic manipulation in the essential background. One possible solution is to generate conditional mutants, such as temperature-sensitive variants (29, 47), for the genes of interest in the essential background, which facilitates the functional testing of candidate modifiers. Another possibility is to take advantage of

recently developed CRISPR-Cas9–based methods that allow direct manipulation of diploid individuals (48–51). For example, in this study, we used a CRISPR-Cas9 plasmid that enables a one-step homozygous deletion of *CYS3* directly in the Y12/Σ1278b hybrid, for which both parental strains were nonviable with deletion of this gene (*Methods*). This strategy, combined with editing-based approaches that enable direct allelic swaps in both haploid and diploid backgrounds (49), should facilitate the systematic and precise identification of modifier variants.

Our study illustrated an example of conditional gene essentiality driven by genetic interactions involving independent and multiallelic modifiers across a natural population, and highlighted the role of rare variants in this phenotype. To gain a deeper insight into the genetic basis of conditional gene essentiality at the species level, more isolate backgrounds need to be explored. With recent technological advances, such as transposon-based saturation mutagenesis (52) and CRISPR-Cas9–based mutation strategies (48–51), high-throughput and parallel exploration of conditional essential genes across multiple strain backgrounds should be achievable in the near future. Systematic identification of the modifiers and their interactions across multiple cases and backgrounds will refine our view of the functional relationship between modifiers and associated primary variants and provide further insights into the molecular basis and the genetic architecture of background-specific conditional phenotypes.

Methods

Yeast Strain Construction. Strains used in this study are detailed in Dataset S2. Natural isolates originated from diverse ecological and geographical sources were kindly provided by Joseph Schacherer, University of Strasbourg, Strasbourg, France (31, 34). Heterozygous deletion mutants in the S288c and Σ1278b backgrounds are described in Dowell et al. (23). To enable targeted gene disruption in natural yeast strains, we engineered deletion of the *URA3* gene (*ura3Δ0*), using a CRISPR-Cas9–based strategy (see below). Deletions and allele replacements of *CYS3*, *CYS4*, *OPT1*, and *MET1* in the various backgrounds were performed using standard PCR-based homologous recombination (53). Gene deletion was performed by transforming a fragment of *URA3* with 50-bp flanking homology regions targeting the gene of interest. The deletion mutants were then transformed with the desired allelic variants, with ∼200 bp up- and downstream homology regions targeting the same locus, and selected on 5-FOA. The correct replacement mutants were confirmed using PCR based on the amplicon sizes. The Y12/Σ1278b hybrid with a single deletion of *CYS3* was generated by mating haploid wild-type Y12 and Σ1278b *Δcys3* through rescue crossing (see below). A Y12/Σ1278b hybrid with homozygous deletion of *CYS3* was constructed using a plasmid expressing Cas9 and a *CYS3*-specific guide RNA with repair fragment homologous to the targeted locus (see below for details).

Media and Culture Conditions. Yeast strains were grown on standard rich media YPD (1% yeast extract, 2% peptone, 2% glucose) with 2% agar for culturing on plates. Selection of deletion alleles marked with *kanMX* or *natMX* markers was done on YPD supplemented with 200 μg/mL of G418 or 100 μg/mL of nourseothricin, respectively. Rich media with galactose YPGAL was used for induction of Cas9 for relevant gene deletion experiments (1% yeast extract, 2% peptone, 2% galactose). Synthetic dropout media SD – uracil (yeast nitrogen base with ammonium sulfate without amino acids 6.7 g/L, uracil dropout mix 2 g/L, glucose 20 g/L, and agar 20 g/L) and synthetic complete media with 5-FOA, SC +5-FOA (yeast nitrogen base with ammonium sulfate without amino acids 6.7 g/L, complete amino acids mix 2 g/L, glucose 20 g/L, 5-FOA 1 g/L and agar 20 g/L) were used for allele replacements. Sporulation was induced on potassium acetate plates (1% potassium acetate, 2% agar). All tetrad dissections were performed on YPD.

Hybrid Generation and Rescue Crossing Strategy. S288*c*/Σ1278b hybrids heterozygous for deletion of conditional essential genes were constructed by crossing a wild-type haploid individual from the background in which the gene was essential with the corresponding deletion mutant constructed in the background in which the gene was nonessential. To generate hybrids homozygous for deletion of a conditional essential gene, we performed rescue crossing. This protocol involved sporulation of a diploid heterozygous for an essential gene, followed by tetrad dissection. In parallel, a haploid strain carrying a deletion of the same gene in the background in which the gene was not essential was grown to exponential phase, and single cells were isolated from the culture using a dissection microscope. Single unbudded cells were individually aligned to each spore that was previously dissected from the essential background. After 3–5 h of incubation at 30 °C, a fraction of all tested pairs formed zygotes, which were isolated using micromanipulation and allowed to form colonies. Strains homozygous for deletion of the targeted gene were then identified by PCR amplifications of the relevant locus and by genetic analysis of segregation of the deletion marker.

One-Step Homologous Gene Deletion in Diploid Strains Using CRISPR-Cas9. We developed plasmid constructs for direct homologous gene deletion in diploid individuals using CRISPR-Cas9. For these experiments we constructed a plasmid expressing the Cas9 gene from *Streptococcus pyogenes* (spCas9) from the inducible *GAL1* promoter, a guide RNA, and scaffold sequences with a SNR52 promoter (50), as well as a deletion fragment carrying the *natMX* marker bordered by ∼200 bp of sequence homologous to the targeted genes. The plasmid backbone contains the *URA3* and *kanR* markers, the yeast *CEN6* sequence fused to an autonomous replication sequence (ARS), as well as an ampicillin resistance marker and an *Escherichia coli* replication origin site from the standard pBluescript SK II (+) plasmid. For all wild diploid isolates used in this study (Dataset S2), a plasmid with guide RNA targeting the *URA3* locus (GGGTCAACAGTATAGAACCG) and a repair fragment without the *natMX* marker (*ura3Δ0*) was constructed. Strains were transformed and selected on YPD+G418. The transformants were transferred to liquid galactose media YPGAL and incubated overnight at 30 °C. Individuals with homozygous deletion of *URA3* and loss of the deletion plasmid were selected on SC +5-FOA. For homozygous deletion of *CYS3* in the Y12/Σ1278b hybrid and the diploid Y12 with a single copy replacement of *MET1* (Y12 $MET1^{Y12}/MET1^{\Sigma 1278b}$), a plasmid with guide RNA targeting the *CYS3* locus (TATTGAGCGTTCTCTAAAGG) and a deletion fragment with *natMX* was constructed. The same induction procedure was used and deletion mutants were selected on SC +5FOA +clonNAT. Individuals carrying homozygous deletion of *CYS3* were confirmed using PCR.

Bulk Segregant Analysis and Whole-Genome Sequencing. Offspring pools from various crosses were selected based on the segregation patterns. Selected individuals originated from independent tetrads and were cultured separately, then pooled together based on equal optical density readings at 600 nm. The DNA of pooled segregants was extracted using QIAGEN DNeasy Blood & Tissue kits and sequenced using the Illumina Hiseq platform, with a coverage of 50×. Reads obtained were mapped to the S288c genome using the Burrows–Wheeler Aligner (BWA, version 0.7.15) with the –mem option (54). Variant calling was performed using SAMTools (version 1.3.1) with default parameters (55). Single nucleotide polymorphism positions with a coverage lower than 20× were removed from subsequent analysis. The allele frequency of S288c at each polymorphic position was extracted from the variant calling file using custom made R scripts. For the pool from the Σ1278b and Y12 cross, only positions that differed between the two parental strains were considered and the allele frequency of Y12 was calculated by counting the reads that corresponded to the respective allelic version. To simplify the analysis, a kernel regression model was fitted to the allele frequency data with a 20-kb window, using the ksmooth function in R (package "stats"). Regions with smoothed allele frequency higher than 0.75 or lower than 0.30, corresponding to ±2.5× SD from the mean allele frequency, were considered as significant. Regions that exceeded the enrichment cutoffs but spanned less than 10 kb in length were considered likely to reflect sequencing noise related to genomic regions with low parental divergence and were not considered as significant. An enriched genomic region on the left telomere of chromosome VI related to the S288*c*/Σ1278b *cys3Δ/cys3Δ* segregant pool (Fig. 1*B* and *SI Appendix*, Fig. S1*A*) was manually removed due to a loss-of-heterozygosity event in favor of the S288c alleles in this region, which was unrelated to the conditional essential phenotype.

Plasmid Construction. Centromeric plasmids that carry combinations of *OPT1* promoter and protein encoding region were generated using multifragment cloning directly in the diploid Σ1278b background heterozygous for a *CYS3* or *CYS4* deletion allele. The plasmid backbone contains the yeast *CEN6-ARS*, an ampicillin resistance marker and an *E. coli* replication origin site from a standard pBluescript SK (+) plasmid. Promoter regions, corresponding to 1 kb upstream of the *OPT1* gene, were amplified from S288c and Σ1278b, as well as the coding regions of *OPT1* with their native terminators. The *URA3* marker was amplified from FY4, a prototroph strain isogenic to S288c. All fragments, each with an overlap of 50 bp, were cotransformed into Σ1278b *CYS3/cys3Δ* and Σ1278b *CYS4/cys4Δ*, with the desired combinations.

GENETICS

Transformants carrying the functional plasmids were selected on SD −uracil, and meiotic progeny were then isolated by tetrad dissection.

Sequence Mining for Isolates Carrying Potential Modifier Variants. Functional effect annotations were obtained for 1,011 yeast isolates described in Peter et al. (31). All isolates were surveyed for the presence of the specific modifier variants identified in Σ1278b (*OPT1*) and Y12 (*MET1*). For potential loss-of-function variants associated with the cysteine biosynthesis pathway, annotations for all genes involved were investigated across 1,011 isolates, and variants with predicted high impacts, including loss of start codon, gain of stop codon, and frameshift, were further analyzed. High-impact annotations that occurred within the last three amino acid residues were not considered to be loss-of-function variants; only annotations within the protein encoding regions were considered. The neighbor-joining tree of 31 isolates used in this study was generated using the R package "ape" (56). The distance matrix was calculated based on 332,722 polymorphic sites using the dist.gene function. Tree file was generated using the nj function and plotted in R.

Accession Numbers. All short reads data generated in this study have been deposited to the NCBI Sequence Read Archive under the BioProject ID PRJNA493856 (57).

ACKNOWLEDGMENTS. We thank Joseph Schacherer, Michael Costanzo, and José Rojas Echenique for comments on the manuscript. Functional genomics work in the C.B. and B.J.A. laboratories is supported primarily by the Canadian Institutes for Health Research Grants FDN-143264 and FDN-143265, the National Institutes of Health Grant R01HG00583, and the Ontario Ministry of Research Innovation and Science Grant RE07-037. C.B. holds a Canada Research Chair (tier 1) in Proteomics, Bioinformatics, and Functional Genomics. C.B. and B.J.A. are senior fellows and co-directors of the Canadian Institutes for Advanced Research Genetic Networks Program.

1. Cooper DN, Krawczak M, Polychronakos C, Tyler-Smith C, Kehrer-Sawatzki H (2013) Where genotype is not predictive of phenotype: Towards an understanding of the molecular basis of reduced penetrance in human inherited disease. *Hum Genet* 132: 1077–1130.
2. Chandler CH, Chari S, Tack D, Dworkin I (2014) Causes and consequences of genetic background effects illuminated by integrative genomic analysis. *Genetics* 196: 1321–1336.
3. Sackton TB, Hartl DL (2016) Genotypic context and epistasis in individuals and populations. *Cell* 166:279–287.
4. Chow CY (2016) Bringing genetic background into focus. *Nat Rev Genet* 17:63–64.
5. Mullis MN, Matsui T, Schell R, Foree R, Ehrenreich IM (2018) The complex underpinnings of genetic background effects. *Nat Commun* 9:3548.
6. Hou J, van Leeuwen J, Andrews BJ, Boone C (2018) Genetic network complexity shapes background-dependent phenotypic expression. *Trends Genet* 34:578–586.
7. Chen R, et al. (2016) Analysis of 589,306 genomes identifies individuals resilient to severe Mendelian childhood diseases. *Nat Biotechnol* 34:531–538.
8. Fournier T, Schacherer J (2017) Genetic backgrounds and hidden trait complexity in natural populations. *Curr Opin Genet Dev* 47:48–53.
9. Domingo J, Diss G, Lehner B (2018) Pairwise and higher-order genetic interactions during the evolution of a tRNA. *Nature* 558:117–121.
10. Chow CY, Kelsey KJP, Wolfner MF, Clark AG (2016) Candidate genetic modifiers of retinitis pigmentosa identified by exploiting natural variation in *Drosophila*. *Hum Mol Genet* 25:651–659.
11. Steinberg MH, Sebastiani P (2012) Genetic modifiers of sickle cell disease. *Am J Hematol* 87:795–803.
12. Dorfman R (2012) Modifier gene studies to identify new therapeutic targets in cystic fibrosis. *Curr Pharm Des* 18:674–682.
13. Cutting GR (2010) Modifier genes in mendelian disorders: The example of cystic fibrosis. *Ann N Y Acad Sci* 1214:57–69.
14. Botstein D (2015) *Decoding the Language of Genetics* (Cold Spring Harbor Lab Press, Cold Spring Harbor, NY).
15. Jin SC, et al. (2017) Contribution of rare inherited and de novo variants in 2,871 congenital heart disease probands. *Nat Genet* 49:1593–1601.
16. Forsberg SKG, Bloom JS, Sadhu MJ, Kruglyak L, Carlborg Ö (2017) Accounting for genetic interactions improves modeling of individual quantitative trait phenotypes in yeast. *Nat Genet* 49:497–503.
17. Chandler CH, et al. (2017) How well do you know your mutation? Complex effects of genetic background on expressivity, complementation, and ordering of allelic effects. *PLoS Genet* 13:e1007075.
18. Taylor MB, Ehrenreich IM (2014) Genetic interactions involving five or more genes contribute to a complex trait in yeast. *PLoS Genet* 10:e1004324.
19. Edwards MD, Symbor-Nagrabska A, Dollard L, Gifford DK, Fink GR (2014) Interactions between chromosomal and nonchromosomal elements reveal missing heritability. *Proc Natl Acad Sci USA* 111:7719–7722.
20. Kim D-U, et al. (2010) Analysis of a genome-wide set of gene deletions in the fission yeast Schizosaccharomyces pombe. *Nat Biotechnol* 28:617–623.
21. Blomen VA, et al. (2015) Gene essentiality and synthetic lethality in haploid human cells. *Science* 350:1092–1096.
22. Boutros M, et al.; Heidelberg Fly Array Consortium (2004) Genome-wide RNAi analysis of growth and viability in Drosophila cells. *Science* 303:832–835.
23. Dowell RD, et al. (2010) Genotype to phenotype: A complex problem. *Science* 328: 469.
24. Hart T, et al. (2015) High-resolution CRISPR screens reveal fitness genes and genotype-specific cancer liabilities. *Cell* 163:1515–1526.
25. Vu V, et al. (2015) Natural variation in gene expression modulates the severity of mutant phenotypes. *Cell* 162:391–402.
26. Wang T, et al. (2015) Identification and characterization of essential genes in the human genome. *Science* 350:1096–1101.
27. Kamath RS, et al. (2003) Systematic functional analysis of the Caenorhabditis elegans genome using RNAi. *Nature* 421:231–237.
28. Paaby AB, et al. (2015) Wild worm embryogenesis harbors ubiquitous polygenic modifier variation. *eLife* 4:e09178.
29. Costanzo M, et al. (2016) A global genetic interaction network maps a wiring diagram of cellular function. *Science* 353:aaf1420.
30. van Leeuwen J, et al. (2016) Exploring genetic suppression interactions on a global scale. *Science* 354:aag0839.
31. Peter J, et al. (2018) Genome evolution across 1,011 Saccharomyces cerevisiae isolates. *Nature* 556:339–344.
32. Ono BI, et al. (1999) Cysteine biosynthesis in Saccharomyces cerevisiae: A new outlook on pathway and regulation. *Yeast* 15:1365–1375.
33. Bourbouloux A, Shahi P, Chakladar A, Delrot S, Bachhawat AK (2000) Hgt1p, a high affinity glutathione transporter from the yeast Saccharomyces cerevisiae. *J Biol Chem* 275:13259–13265.
34. Schacherer J, Shapiro JA, Ruderfer DM, Kruglyak L (2009) Comprehensive polymorphism survey elucidates population structure of Saccharomyces cerevisiae. *Nature* 458:342–345.
35. Pruyne D, et al. (2002) Role of formins in actin assembly: Nucleation and barbed-end association. *Science* 297:612–615.
36. Bloom JS, Ehrenreich IM, Loo WT, Lite T-LV, Kruglyak L (2013) Finding the sources of missing heritability in a yeast cross. *Nature* 494:234–237.
37. Albert FW, Treusch S, Shockley AH, Bloom JS, Kruglyak L (2014) Genetics of single-cell protein abundance variation in large yeast populations. *Nature* 506:494–497.
38. Ehrenreich IM, et al. (2010) Dissection of genetically complex traits with extremely large pools of yeast segregants. *Nature* 464:1039–1042.
39. Fay JC (2013) The molecular basis of phenotypic variation in yeast. *Curr Opin Genet Dev* 23:672–677.
40. Hou J, Schacherer J (2017) Fitness trade-offs lead to suppressor tolerance in yeast. *Mol Biol Evol* 34:110–118.
41. Hamilton BA, Yu BD (2012) Modifier genes and the plasticity of genetic networks in mice. *PLoS Genet* 8:e1002644.
42. Liti G, et al. (2009) Population genomics of domestic and wild yeasts. *Nature* 458: 337–341.
43. Yue J-X, et al. (2017) Contrasting evolutionary genome dynamics between domesticated and wild yeasts. *Nat Genet* 49:913–924.
44. Strope PK, et al. (2015) The 100-genomes strains, an *S. cerevisiae* resource that illuminates its natural phenotypic and genotypic variation and emergence as an opportunistic pathogen. *Genome Res* 25:762–774.
45. Hou J, et al. (2016) The hidden complexity of mendelian traits across natural yeast populations. *Cell Rep* 16:1106–1114.
46. Hou J, Friedrich A, Gounot J-S, Schacherer J (2015) Comprehensive survey of condition-specific reproductive isolation reveals genetic incompatibility in yeast. *Nat Commun* 6:7214.
47. Tan G, Chen M, Foote C, Tan C (2009) Temperature-sensitive mutations made easy: Generating conditional mutations by using temperature-sensitive inteins that function within different temperature ranges. *Genetics* 183:13–22.
48. Sadhu MJ, et al. (2018) Highly parallel genome variant engineering with CRISPR-Cas9. *Nat Genet* 50:510–514.
49. Sharon E, et al. (2018) Functional genetic variants revealed by massively parallel precise genome editing. *Cell* 175:544–557.e16.
50. DiCarlo JE, et al. (2013) Genome engineering in Saccharomyces cerevisiae using CRISPR-Cas systems. *Nucleic Acids Res* 41:4336–4343.
51. Smith JD, et al. (2016) Quantitative CRISPR interference screens in yeast identify chemical-genetic interactions and new rules for guide RNA design. *Genome Biol* 17: 45.
52. Michel AH, et al. (2017) Functional mapping of yeast genomes by saturated transposition. *eLife* 6:e23570.
53. van Leeuwen J, Andrews B, Boone C, Tan G (2015) Rapid and efficient plasmid construction by homologous recombination in yeast. *Cold Spring Harb Protoc* 2015: t085100.
54. Li H, Durbin R (2009) Fast and accurate short read alignment with Burrows-Wheeler transform. *Bioinformatics* 25:1754–1760.
55. Li H (2011) A statistical framework for SNP calling, mutation discovery, association mapping and population genetical parameter estimation from sequencing data. *Bioinformatics* 27:2987–2993.
56. Paradis E, Claude J, Strimmer K (2004) APE: Analyses of phylogenetics and evolution in R language. *Bioinformatics* 20:289–290.
57. Hou J (2019) Conditional gene essentiality in yeast. The Sequence Read Archive/NCBI-NIH. Available at https://www.ncbi.nlm.nih.gov/bioproject/PRJNA493856. Deposited September 28, 2018.